Supporting Information

Self-assembly three-dimensional liver organoids: virtual reconstruction via endocytosed polymer dots for refactoring the fine structure

Ze Zhang,[a] Yuyang Wu,[b] Zhilu Xuan,[c] Haotian Xu, [a] Shengyan Yin,*[b] and Zihui Meng*[a]

[a] *Department of Hepatobiliary-Pancreatic Surgery, China-Japan Union Hospital of Jilin University, Jilin University, No.126 Xiantai Street, Changchun, Jilin 130000, P.R. China*
[b] *State Key Laboratory of Integrated Optoelectronic, College of Electronic Science and Engineering, Jilin University, No.2699 Qianjin Street, Changchun, Jilin 130012, P. R. China*
[c] *Department of Obstetrics & Gynecology, The First Hospital of Jilin University, Changchun, Jilin 130012, P. R. China*
E-mail address: syyin@jlu.edu.cn; zhmeng@jlu.edu.cn

Contents

Author Contributions

Z.Z Conceptualization: Supporting; Data curation: Lead; Formal analysis: Lead; Writing – original draft: Lead; Writing – review & editing: Supporting
Wu Y.Y Data curation: Supporting; Formal analysis: Supporting
Xuan Z.L Data curation: Supporting; Formal analysis: Supporting; Specimen collection: Supporting
Xu H.T Conceptualization: Supporting; Specimen collection: Supporting
Yin S.Y Conceptualization: Supporting; Data curation: Lead; Formal analysis: Lead; Writing – original draft: Lead; Writing – review & editing: Supporting
Meng Z.H Conceptualization: Supporting; Data curation: Supporting; Formal analysis: Supporting; Writing – review & editing: Supporting

Materials and Methods

Materials.

The conjugated polymers used in this study are polyfluorene derivative poly [(9,9-dioctylfuranyl-2,7-diyl)-alt-co-(1,4-benzo-{2,1',3}-thiadiazole)] (PFBT, MW:10000-100000, Xi'an Polymer Light Technology Company). Poly{[2,7-(9-(20-ethylhexyl)-9-hexyl-fluorene])-alt-[5,50-(40,70-di-2-thienyl-20,10,30-benzothid-iazole)]} (PFDTBT, MW > 10000, PDI < 4, Derthon Optoelectronic Materials Science Technology Co Ltd). Poly (styrene-co-maleic anhydride) (PSMA, cumene terminated, average molecular weight 1700, styrene content 68 %, Sigma-Aldrich). Tetrahydrofuran (THF, anhydrous, 99.9 %, Beijing Chemical Works). Ultrapure water prepared by Milli-Q (Millipore) device was used in all experiments.[1, 2]

Characterizations of the Pdots and R8-Pdots

The absorption spectrum was measured on an UV-2600 UV-Vis spectrophotometer (Shimadzu). Fluorescence spectra were analyzed on an F-4500 spectrophotometer (Hitachi). Dynamic light scattering (DLS) and Zeta potential analysis was carried out on ZLS (NANZS, Malvern).

Cell Culture

Culture of MSCs: Umbilical cord-derived MSCs were obtained from the umbilical cord of 23 pregnant women (umbilical cords with good anatomy can be used to extract HUVECs) who underwent a cesarean section & natural labor and signed informed consent at The Ethics Committee approved this study of the China-Japan Union Hospital of Jilin University (No.2021081021). The collected umbilical cords were washed with 75 % medical alcohol, 0.9 % normal saline, and PBS. The cleaned umbilical cords were cut into pieces with ophthalmic scissors (each size of nearly one cubic millimeter) and cultured in 10 cm^2 petri dishes. After nearly 4-7 days, the primary MSCs were dissociated from the umbilical cord and placed adherently in the petri dish. The MSCs were incubated in Dulbecco's modified Eagle medium (MEN medium, Biological Industries, BI®) containing no antibiotics but with 5 % UltraGRO-Advanced (No. Hpcfdcrl05, Helios®, USA) in a humidified incubator at 37 °C with 5 % CO_2 (after configuration, biological sterile filters with pore sizes of 0.32 μm and 0.22 μm were used for filtration, Millipore, USA).[3] The medium was refreshed every 2–3 days. In this study, the MSCs between passages 3 and 7 were employed.[4]

Culture of HUVECs: Umbilical vein endothelial-derived HUVECs were obtained from the umbilical cord of 27 pregnant women who underwent a cesarean section & natural labor and signed informed consent at the China-Japan Union Hospital of Jilin University (the donor had no pregnancy complications or genetic diseases). Please refer to the above procedure for the first step of umbilical cord cleaning. First, the umbilical vein lumen was washed with 0.9 % normal saline and PBS. Subsequently, a mixture of 0.1 % collagenase and 0.25 % trypsin (Gibco; Thermo Fisher Scientific, MA, USA) was used to fill the venous lumen at both ends of the clip. Next, the umbilical cord was immersed in 0.9 % warm saline (37 ℃). The cell mass at the bottom of the centrifuge tube was extracted after centrifugation (1500 rpm*10 min). Endothelial Cell Medium (ECM, ScienCell, Catalog #1001), comprising 500 mL of basal medium, 25 mL of FBS (Cat. #0025), 5 mL of Endothelial Cell Growth Supplement (ECGS, Cat. #1052), and 5 mL of penicillin/streptomycin solution (P/S, Cat. #0503), was employed to cultivate HUVECs in vitro[5]. The medium was refreshed every 2 days. Furthermore, the HUVECs between passages 3 and 7 were adopted.[6]

Extraction of Wharton's Jelly: Remove the adventitia and internal blood vessels from the washed umbilical cord, cut the resting tissue into pieces with ophthalmic scissors, and place it in a 50 mL centrifuge tube with vigorous shaking. Stop when the PBS solution in the centrifuge tube turns cloudy and pale yellow. Discard the sediment at the bottom, only retain the suspension at the top, and place it at -20 °C for at least six repeated freeze-thaw cycles. Melting in a 4 °C refrigerator before use, extract only the pale-yellow PBS suspension, pass it through molecular sieves, and then dilute Wharton's Jelly to 1 mg/mL with PBS.[7, 8]

Adult human liver cells: The above cells were largely derived from voluntary donations from three patients with hepatic hemangiomas. The Ethics Committee approved this study of the China-Japan Union Hospital of Jilin University (No.20211130008 and No.20221208017). When the patient's tissues were surgically removed, we only extracted normal liver tissues with good peripheral anatomy. Subsequently, the tissue block was washed with pre-cooled 0.9 % normal saline, PBS, etc. The tissues were cut into 1 mm^3 piece with ophthalmic scissors and then ground with glass slides. After washing with PBS again, 0.25 % trypsin and 0.1 % collagenase (Gibco; Thermo Fisher Scientific, MA, USA) were added for 20 min (37 °C). After the serum-containing culture medium was added to terminate the digestion, the cells passed through a 300-mesh cell strainer (Millipore, USA), and the filtered liquid was placed in a centrifuge (500 g*10 min). The extracted cells were cultured in a petri dish and then cultured in DuIbecco's Modified EagIe's medium/Nutrient Mixture F-12 (DMEM/F12 medium, Gibco®) containing 5 % Bovine Calf Serum (Biological Industries, BI®). Subsequently, the cultured primary cells were subjected to flow sorting, and only the liver epithelium cells were retained.[9]

As for the collection of single-cell suspensions, liver organoid cell clusters and isolated liver tissues were dissociated into single cells by the treatment of TrypLE Express (Gibco®) for 10 min at 37 °C; the cell concentration after treatment was 1 × 10^6 cells/mL. After PBS wash twice, the single cells were incubated with Cy5-conjugated HepPAR1 antibody (anti-hepatocyte specific antigen, Sigma) at room temperature (24 °C) for 30 min. After PBS wash, cell sorting was performed by Flow Cytometry (BD Biosciences). Analysis was performed by BD instrument supporting software and FlowJo (FlowJo, LLC).[10]

Cell surface antigen phenotyping and Cytotoxicity

The phenotype characteristics of cultured MSCs (P3-P7) and MSCs co-cultured with PFBT Pdots/R8-PFBT Pdots were identified using flow cytometry. First, in accordance with the description published previously, the cells were treated with 1 mL of Trypsin-EDTA (Trypsin-Ethylene Diamine Tetraacetic Acid) at 37 °C for 5~10 min. Next, the cells were resuspended in 10 mL of PBS and centrifuged at 1,000 × g for 5 min. Afterward, the cells were resuspended in flow cytometry buffer (phosphate buffered saline containing two mM of EDTA and 10 % blocking reagent) at 1 × 10^6 cells/mL. Next, 50~100 μL of cell suspension was added to a 1.5 mL tube and then incubated with 2 μL fluorescent antibodies [Mouse Anti-Human CD34-PE (550761), CD45-FITC (555482), CD29-PE (555443), CD73-PE (550257), CD105-PE (560839), CD90-FITC (555595),[11, 12] Rat Anti-Mouse IgG1-PE (550083) and Anti-Mouse IgG1-FITC (553443). All antibodies originated from BD® Biosciences.] and the homotypic controls were performed on ice (0~4 °C) for 45 min. Next, the cells were washed with flow cytometry buffer, fixed in 10% formalin, and stained with 50~100 μL of 0.2 % viability dye solution. After incubation at ambient temperature for 15 min, the cells were washed twice with flow cytometry buffer and filtered through a 70 μm

cell strainer. The positive rate of antigen was examined using a flow cytometry system (Guava easyCyte8HT, EMD Millipore, Billerica, MA).

Cell viability text: Cell Counting Kit-8 (CCK-8) -- Cells that should be tested were seeded in 96-well plates at 5×10^3 cells/well. CCK-8 reagent (10 μL; Dojin Laboratories, Japan) was added to the respective well at 24 h and then incubated for another 4 h at 37 °C. The cell viability was examined by measuring the optical density (OD) value at 450 nm with a Microplate Reader (Bio-Rad, USA).[13] Five sets of accessory wells were set for the respective sample, and the middle three sets of data were employed for statistical analysis. Furthermore, three additional sets of accessory pores without cell implantation were required as the blank control groups due to the light absorption and emission properties of the fluorescent dye.

Cell immunostaining: Primary HUVECs and cells at different time points of induction differentiation were fixed overnight at 4 °C in 4 % paraformaldehyde, and the stained cells were treated with 0.1% Triton X-100 (No. P1080, Solarbio®). Immunostaining was preceded through autoclave antigen retrieval in citrate buffer (pH 6.0). The primary antibodies were anti-human: anti-hepatocyte specific antigen (anti-HepPAR1, Sigma, Cat No.246R-14-RUO), anti-albumin (Abcam, Cat No.ab207327), anti-alpha 1 fetoprotein (Abcam, Cat No.ab169552) and anti-von Willebrand Factor (anti-vWF, Santa, Cat No.sc-53466), anti-CD31 (platelet/endothelial cell adhesion molecule, PECAM-1) monoclonal (anti-PECAM-1/ anti-CD31, Abcam)[10, 14]. The tissue sections were incubated with the secondary antibody (Life Technologies) for 1 h at ambient temperature, followed by DAPI (2-(4-Amidinophenyl)-6-indolecarbamidine dihydrochloride) (Sigma, USA) nuclear staining. The images were captured using a Nikon A1R confocal laser scanning microscopy (Japan).

Validate the "skeleton" function of primary HUVECs

We replaced the extracted primary venous endothelial cells with bioengineered immortal endothelial cells (PUMC-HUVEC-T1, Homo sapiens, Cat No. PNS-HC-65, ProCell®), which have poor adhesion and lack part of the molecular phenotype of the primary cells, to verify this finding further. The results suggest that the liver organoid structure with spatial structure could not be formed in vitro, and the general shape only stayed in the schematic diagram of Figure 6A 24 h film-forming state (See Supplementary Figure S6 for details).

Untargeted metabolomic analysis

Sample preparation: The culture medium was discarded. It was washed three times with PBS. The bottom of the dish was immersed with liquid nitrogen for 30 s to quench adherent cells. Subsequently, 500 μL (the amount was adjusted in accordance with the bottom area of the petri dish) of pre-cooled methanol and DEPC water mixed solution (4:1, v/v) (chromatographic grade methanol, Cat No. PHR1372, Sigma-Aldrich), (DNase/RNase-Free Delionized Water, DEPC water, Cat No. RT121-02, Tiangen®) was added. Afterward, a cell scraper was employed to scrape cells from the bottom of the dish and store them in dry ice. Shanghai PersonalBio Biotechnology Co., Ltd. will undertake subsequent non-targeted metabolomic testing in mainland China (Contract No.MI202110004/MAP2021112176). After slow thawing at 4 °C, 1 mL methanol: acetonitrile: water (2:2:1, v/v) was added for complete vortex mixing. The sonication was performed at low temperatures. The sample was incubated at the temperature of -20 °C for 1 h at 13000 rpm for the precipitation of proteins. The centrifugation was achieved for 15 min at the temperature of 4 °C. The supernatant was collected, freeze-dried, and maintained at -80 °C until use. 100 μL of

acetonitrile aqueous solution (acetonitrile: water = 1:1, v/v) was added for reconstitution, vortexed, centrifuged at 14,000 g for 15 min at 4 °C to conduct mass spectrometry analysis. Furthermore, the supernatant was collected, and then the injection was investigated.[15]

Spectrum analysis: The samples were separated by an Agilent 1290 Infinity LC ultra-high performance liquid chromatography (UHPLC) HILIC column. The column temperature was 25 °C. The flow rate was 0.5 mL/min; the injection volume was 2 μL. Mobile phase composition A: water + 25 mM ammonium acetate + 25 mM ammonia, B: acetonitrile. The gradient elution program was as follows: 0 --- 0.5 min, 95 %; B: 0.5 --- 7 min; B linearly changes from 95 % to 65 %: 7 --- 8 min; B from 65 % linear change to 40 %; 8---9 min, B maintained at 40 %; 9---9.1 min, B linearly changed from 40 % to 95 %; 9.1---12 min, B held at 95 %. The samples were placed in an autosampler at 4°C throughout the analysis. The samples were continuously analyzed in random order to avoid the effect of the instrument detection signal fluctuation. In addition, QC samples were inserted into the sample queue to monitor and evaluate the stability of the system and the reliability of the experimental data.[16]

Mass spectrometry identification: Electrospray Ionization (ESI) was employed for detection in positive and negative ion modes, respectively. The samples were separated by UHPLC, and then mass spectrometry analysis was conducted on the samples using a Triple TOF 6600 Mass Spectrometer (AB SCIEX). The samples were separated by an Agilent 1290 Infinity LC ultra-high performance liquid chromatography system (UHPLC) and then analyzed with a Triple TOF 6600 Mass Spectrometer (AB SCIEX) using electrospray ionization (ESI) in positive and negative ion modes, respectively. The ESI source setting parameters included atomizing gas, auxiliary heating gas 1 (Gas1): 60, auxiliary heating gas 2 (Gas2): 60, curtain gas (CUR): 30 psi, ion source temperature: 600 ℃, spray voltage (ISVF) ± 5500 V (both positive and negative modes); the detection range of the primary mass-to-charge ratio: 60-1000 Da, the detection range of the mass-to-charge ratio of the secondary production: 25-1000 Da, the accumulation time of the primary mass spectrometer scan: 0.20 s/spectra. The second mass spectrometry scan accumulation time was 0.05 s/spectra. The second mass spectrum was acquired using the data-dependent acquisition mode (IDA), and the peak intensity value screening mode was adopted. The declustering voltage (DP): ±60 V (both positive and negative modes), collision energy: 35 ± 15 eV. IDA settings were as follows: Dynamically excluded isotope ion range: 4 Da, 10 fragment spectra were collected per scan.[17]

Data analysis: The raw data to mzML format using ProteoWizard, and then the XCMS program was employed for peak alignment, retention time correction, and extraction of peak areas. For the structure identification of metabolites, accurate mass matching (< 25 ppm) and secondary spectrum matching were employed to search the laboratory's self-built database. The integrity of the data was first checked for the data extracted by XCMS. Metabolites with over 50% missing values in the group were removed and not involved in the subsequent analysis. The extreme values were deleted, and the data were normalized to the total peak area to ensure the parallel comparison between samples and metabolites. After processing, the data was input into the software SIMCA-P 16.1 (Umetrics, Umea, Sweden) for pattern recognition. After the data were preprocessed by Pareto-scaling, multi-dimensional statistical analysis was conducted, including unsupervised principal component analysis (PCA) analysis, with a supervised partial minimum. Discriminant Analysis by Squares (PLS-DA) and Orthogonal Partial Least Squares Discriminant Analysis (OPLS-DA). One-dimensional statistical analysis included Student's t-test and fold-of-variation analysis, and R

software (version 3.5.3) was adopted to generate volcano plots.[18] XCMS software was employed to set the parameters as follows: For peak picking, centWave m/z = 25 ppm, peakwidth = c (10, 60), prefilter = c (10, 100). For peak grouping, bw = 5, mzwid =0.025, minfrac = 0.5 were used.

Adipogenic and osteogenic differentiation

MSCs were seeded into 6-well plates (Corning Inc., Corning, NY) at 2 × 10^4 cells/ well in adipogenic induction medium containing 10 μg/mL of insulin, 500 μM of 3-isobutyl-1-methylxanthine, 100 μM of indomethacin, 1 μM of dexamethasone, and 10 % fetal bovine serum (Gibco) (all from Sigma-Aldrich, St Louis, MO). The fresh medium was replaced every 3 days. After 21 days, Oil Red-O (Sigma-Aldrich) staining was used to identify the intracellular accumulation of lipid-rich vacuoles. In brief, cells were fixed with 4 % paraformaldehyde for 30 min, washed with phosphate buffered saline, and stained with a working solution of 0.3 % Oil Red-O in phosphate buffered saline for 20 min. For osteogenesis, after preparation with 0.1 μM of dexamethasone (Sigma-Aldrich), 0.2 μM of ascorbic acid 2-phosphate (Sigma-Aldrich), 10 mM of glycerol 2-phosphate (Sigma-Aldrich), and 10 % fetal bovine serum, and fixation cells were stained with Alizarin red S (Fluka Buchs SG, Switzerland).[19]

Agarose gel electrophoresis

The mold was washed and assembled, and TAE (1×) buffer (No. T1060, 50×, Solarbio®) was configured. 0.5 g of agarose powder was weighed within an Erlenmeyer Flask, and 50 mL of TAE (1×) buffer was added. The solution was heated for a complete dissolution of the agarose, and the gel concentration reached 0.5%. With the decrease of the solution temperature to nearly 60 ℃, 2 μL EB (10 mg/mL) (Cat No. R22214, Shyuanye®) was added and then well shaken. Since the overall charge character of the modified probe was unknown, the position of the sample filling hole was opened at the half-fold midline of the agarose gel, such that probes with different charge properties were scattered in different directions under the action of the electric field force. The solution was rapidly added to the assembled mold. A clean pipette tip was adopted to take out the bubbles in the mold cavity and place them in a dark box for 40 min. Subsequently, the electrophoresis gel was taken out and then placed in the electrophoresis tank. An appropriate amount of TAE (1×) buffer was introduced into the electrophoresis tank. The sample (Pdots, R8-Pdots, R8-Pdots+EDC) was mixed with Loading Buffer (No.9157, Takarabiomed®) at an appropriate ratio, and the 10 μL sample was loaded. The loading volume of the DL10000 DNA marker reached 5 μL (No.3584A, Takarabiomed®). Lastly, the nucleic acid electrophoresis instrument was turned on, the program was set to 135 V, and an electrophoresis time was set to 30 min (the bands were identified every 10 min). The band was imaged and archived after the electrophoresis. Next, R8-Pdots and R8-Pdots+EDC were placed in high-frequency ultrasound for 30 min to verify the electrostatic adsorption between R8 and Pdots (20 KHz, 650 W), and the samples should be placed in a 4 °C ice-water mixture for an ultrasound to avoid vigorous shaking that can generate heat to denature the samples.[20] The samples were dropped into the sample wells after ultrasonic vibration, and the above electrophoresis process was repeated.

Quantitative Reverse Transcription-Polymerase Chain Reaction (qRT-PCR)

TRIzol reagent (A33250, Invitrogen, Carlsbad, CA, USA) was adopted to assist overall RNAs isolation. In this study, cDNAs synthesis was achieved using a High-Capacity cDNA Reverse

Transcription Kit (No.4374966, Applied Biosystems, Foster City, CA, USA). For qRT-PCRs, the StepOne Plus Real-Time PCR System was applied, which was assisted by the Power SYBRs Green PCR Master Mix (No.4368577, Applied Biosystems). Internal control included β-actin (ACTB) and U6 (Sangon Biotech®), and relative mRNA expression was calculated using the DDCT method which was normalized to ACTB (as 100 %). 2.0 % agarose gel electrophoresis and melting curve analysis can be conducive to verifying the PCR products. The $2^{\triangle\triangle}$Ct method was employed to analyze the data.[21] The respective test sample had five parallel secondary holes, and the middle three sets of values were used for statistical calculation. The referenced primer sequences are presented in the Supplementary Table 1.

Two-photon Confocal Microscopy Fluorescent Imaging.

The growth of the cell lines MSCs, HUVECs, and Induced differentiation of MSCs were achieved in 12-well microscope chamber slides (1 mg/mL Wharton's Jelly employed to achieve double-surface coating) within the respective media for 80~90 % confluence in 24~48 h. Before the experiments, the cells were cleaned with a prewarmed PBS buffer, and the 15-minute fixing of the cells was performed with 2.5 % glutaraldehyde. Subsequently, the PBS-washed cells were penetrated for 15 min using 0.1 % Triton X-100 (No. P1080, Solarbio®). Next, the cells were cleaned by applying PBS again before nuclear dye DAPI was introduced. Afterward, the samples were cleaned using the flowing PBS (15 min in the respective well), mounted with a nonfluorescent mounting medium, and imaged using confocal laser scanning microscopy. The bio-image retention steps of the liver-organoid section staining were consistent with cell line staining. First, the cultured liver organoid cell clusters were washed three times with warm PBS, followed by 30-minute tissue fixation with an EM (electron microscopy)-specific fixative -2.5 % glutaraldehyde (Cat No. PH9003, Phygene®). The bottom of the petri dish was slightly shaken to avoid residual air bubbles in the cleft of the organoid tissues, and the fixator liquid was used to immerse the tissue. The tissues' ultrathin section should be frozen for 30 min after the tissues' fixation to avoid self-collapse of 3D self-assembled organoids, and the thickness of the respective section was regulated at 5 μm. The number of cells in the respective field of view of the tissue section was identified under a microscope, and the action time of the Triton X-100 was properly extended, or its concentration increased to 0.2 %. To avoid the false positive adsorption of the cell's outer membrane to Pdots, which efflux via vesicles, the sample should be cleaned using flowing PBS before the use of the reagent (ProLong™ Live Anti-Quench Reagent, Thermo Fisher Scientific®, P36975), and the applied PBS was not re-utilized.[1] The remaining part of the process was consistent with cell staining.

Flow Cytometry of apoptosis

Apoptosis of MSCs after co-cultured with PFBT Pdots/R8-PFBT Pdots were determined by flow cytometry with the Annexin V- FITC Apoptosis Detection kit (Solarbio®, China). Stable co-cultured MSCs were washed with cold PBS for three times and made into single-cell suspension in 200μL binding buffer containing 10 μL Annexin V-FITC and 5 μL PI-PE for 30min in the dark. The cell apoptotic rate was analyzed by fluorescence-activated cell sorting (FACS) in a flow cytometer (BD Accuri C6 flow cytometry).

Statistical analysis

The experimental data are expressed as the mean ± standard deviation. Statistical analysis was conducted using SPSS 22.0 statistics program (IBM Corporation, Armonk, NY, USA). The differentially expressed conditions of different classes of mRNAs were analyzed in a range of induction time points using GraphPad Prism 9.0 software (GraphPad Software, Inc. USA). For data conforming to normal distribution and homogeneity of variance, the paired t-test was employed to compare data within a group, while the comparisons were drawn between two groups through the unpaired t-test. A one-way analysis of variance followed by Tukey's post hoc test was adopted for comparison among multiple groups. $P < 0.05$ indicated a difference achieving statistical significance.

Supporting Tables

Table S1. The mRNA Primer Sequence

Name	Sequence (5’ - 3’)
U6-F	CTCGC TTCGG CAGC ACA
U6-R	AACGC TTCAC GAATT TGCGT
GAPDH-F	Sangon Biotech®--Order No.661104-0001
GAPDH-R	
ATCB-F	GGCAT CCTCA CCCTG AAGA
ATCB-R	GAAGG TGTGG TGCCA GATTT
Oct4-F	GAAGC AGAAG AGGAT CACCT TG
Oct4-R	TTCTT AAGGC TGAGC TGCAA G
AFP-F	CTTTG GGCTG CTCGC TATGA
AFP-R	GCATG TTGAT TTAAC AAGCT GCT
ALB-F	AGCCC AACGA TGACT ACTTA CT
ALB-R	ACCCA AGAGT TGATG TCCTT TCT
FOXA1-F	GCAAT ACTCG CCTTA CGGCT
FOXA1-R	TACAC ACCTT GGTAG TACGC C
CAR-F	AGTCA TCGGT CAGAC ACCCT T
CAR-R	GTGCA GCGTT ATCTC CAACA G
HNF4α-F	GTCCC AGCAG ATCAC CTC
HNF4α-R	GGATG TACTT GGCCC ACT
TTR-F	GCTGC ATTTA GTGGC CTCAT T
TTR-R	GCAAG GCATA ACCTG ATGTG G
A1AT-F	CACTA TCACC CTGTG GGCAG
A1AT-R	CACAC TGGCC CCATC ATAGA G
G6PC-F	CCCAG GTTCA CCAGT TCCC
G6PC-R	GCCGT CATTA TGGGC CAGA
CYP7A1-F	AGAAG CATTG ACCCG ATGGA T
CYP7A1-R	AGCGG TCTTT GAGTT AGAGG A

CYP3A4-F	TTCAA CAGAT GATCG ACTCC CA
CYP3A4-R	TTGTG TCATA GGCAG CAAAA ATG
FOXA-2-F	GGAGC AGCTA CTATG CAGAG C
FOXA-2-R	CGTGT TCATG CCGTT CATCC
NANOG-F	TTTGT GGGCC TGAAG AAAAC T
NANOG-R	AGGGC TGTCC TGAAT AAGCA G
SOX17-F	GTGGA CCGCA CGGAA TTTG
SOX17-R	GGAGA TTCAC ACCGG AGTCA
PPARA-F	ATGGT GGACA CGGAA AGCC
PPARA-R	CGATG GATTG CGAAA TCTCT TGG

Table S2. Particle size, zeta potential, position of maximum absorption peak and emission peak of PFBT & PFDTBT Pdots and these R8-Pdots

Term Name	Diameter (nm)	Zeta Potential (mV)	$\lambda_{abs,\,Max}$ (nm)	$\lambda_{em,\,Max}$ (nm)
PFBT Pdots	21.04±1.27	-22.3±1.8	320	560
R8-PFBT Pdots	24.36±1.06	+33.8±1.3	322	560
PFDTBT Pdots	21.04±1.18	-22.8±1.2	386	702
R8-PFDTBT Pdots	28.28±2.23	+34.9±1.5	390	702

Note. R8, octa-arginine

Table S3. Metabolic differences between MSCs and 2D-culture induced differentiation of hepatocyte-like cells.

ID	Fold Change	Log_2 Fold Change
3-phosphoethanolamine	3.379309	1.756728
3-(3,4-dihydroxyphenyl) propanoic acid	0.098175	-3.34851
5-S-Methyl-5-thioadenosine	5.03052	2.330707
6-Methylnicotinamide	50.85944	5.668444
Adenosine	2.110728	1.077741
arg-his	2.014468	1.010399
Bis(2-ethylhexyl) amine	0.149366	-2.74307

Cyclic ADP-ribose	2.118058	1.082742
DL-Alanine	2.97223	1.571546
DL-Glutamic acid	2.574563	1.364328
DL-Homoserine	2.673829	1.418907
D-Sphingosine	2.806064	1.488548
Hydrolyzed fumonisin B1	2.35788	1.23749
L-alpha-Glycerylphosphorylcholine	6.885449	2.783551
L-Glutamic acid	2.987411	1.578896
L-Glutathione (reduced)	2.586331	1.370907
L-Histidine	0.127131	-2.97561
L-Norleucine	0.070031	-3.83587
L-Phenylalanine	0.152732	-2.71093
Nicotinamide adenine dinucleotide (NAD+)	2.406116	1.266706
N-Methylhexanamide	2.110732	1.077744
Platelet-activating factor	0.403264	-1.3102
pyroglutamine	4.987017	2.318177
Tetraacetylethylenediamine	2.654946	1.408683
trans-3-Indoleacrylic acid	0.067319	-3.89283
Uridine 5'-diphosphogalactose	2.955806	1.563552

Table S4. Metabolic differences between 3D-liver organoid cultivation and 2D-culture induced differentiation of hepatocyte-like cells.

ID	Fold Change	Log_2 Fold Change
4-octadecadienamide	2.637661	1.399259
4-Bis(2-phenyl-2-propanyl) phenol	2.197717	1.136006
4-dehydrothiomorpholine-3-carboxylic acid	2.278809	1.18828
4-Oxoproline	2.720808	1.444035
5'-S-Methyl-5-thioadenosine	0.496941	-1.00885
6-Methylnicotinamide	0.470867	-1.08661
Adenosine	0.212016	-2.23775

Adenosine 5-monophosphate	0.342147	-1.54731
Amide C18	0.489655	-1.03016
Bis(2-ethylhexyl) amine	4.57944	2.195171
Bis(4-ethylbenzylidene) sorbitol	0.316497	-1.65974
Citric acid	2.622558	1.390974
D-Maltose	0.283713	-1.81749
DL-Alanine	0.268552	-1.89673
DL-Homoserine	0.437718	-1.19193
Dodecyl sulfate	3.185578	1.671555
L-Norleucine	13.35258	3.739046
L-Phenylalanine	2.888411	1.530276
L-Pyroglutamic acid	2.244423	1.166345
acetamide	2.315779	1.211497
Nicotinamide	2.327816	1.218977
Platelet-activating factor	2.599786	1.378393
pyroglutamine	0.485072	-1.04373
Tetraacetylethylenediamine	0.345046	-1.53514
trans-3-Indoleacrylic acid	2.872702	1.522408
UDP-N-acetylglucosamine	4.589562	2.198356
Uridine 5-diphosphogalactose	0.161774	-2.62795

Table S5. Metabolic differences between 3D-liver organoid cultivation and normal liver tissue cells.

ID	Fold Change	Log_2 Fold Change
4-octadecadienamide	4.111803	2.039771
2-(trimethylammonio) ethyl phosphate	0.025075	-5.31763
4-triol	0.371665	-1.42793
1-Hexadecanoylpyrrolidine	2.01893	1.013591
1-Palmitoyl-2-hydroxy-sn-glycero-3-PE	0.021922	-5.51148
1-Stearoyl-2-hydroxy-sn-glycero-3-PE	0.046688	-4.4208

3-thiazolane-4-carboxylic acid	0.191408	-2.38528
3-diol	0.184187	-2.44076
2-Deoxyguanosine 5'-monophosphate (dGMP)	0.149837	-2.73854
2-methylbutyrylcarnitine	0.10687	-3.22608
3-(3,4-dihydroxyphenyl) propanoic acid	0.042939	-4.54156
4-dihydropyridazin-4-one	5.751285	2.523884
6-Methylnicotinamide	12.2817	3.618438
Acetyl-L-carnitine	0.112337	-3.1541
Adenosine	0.062749	-3.99427
Adenosine 5'-monophosphate	0.097661	-3.35607
arg-his	6.158139	2.622494
Betaine	0.043758	-4.5143
Choline	0.194871	-2.35941
Citric acid	0.261523	-1.93499
Creatine	0.156169	-2.67882
D-Pipecolinic acid	0.298929	-1.74212
DL-Alanine	0.038008	-4.71754
DL-Glutamic acid	0.166588	-2.58564
DL-Glutamine	0.425841	-1.23161
DL-Homoserine	0.392969	-1.34751
DL-Malic acid	0.078305	-3.67476
Dodecyl sulfate	0.023868	-5.38878
D-Sphingosine	0.242446	-2.04426
Glycerophosphoglycerol	0.164651	-2.60252
Glycocholic acid	0.005676	-7.46087
Hypoxanthine	0.009902	-6.65809
Inosine	0.020338	-5.61965
Carnitine	0.044987	-4.47434
L-alpha-Glycerylphosphorylcholine	0.05159	-4.27677

Lauramide	3.726807	1.89794
L-Glutamic acid	0.070455	-3.82715
L-Glutathione (reduced)	0.286208	-1.80486
L-Histidine	0.061246	-4.02923
L-Norleucine	0.285667	-1.80759
L-Phenylalanine	0.345082	-1.53499
lysophosphatidylethanolamine	0.149937	-2.73757
methadone-d9	8.670384	3.116096
Methyl palmitate	0.3841	-1.38044
MFCD22416941	0.014244	-6.13351
N-Diisopropylethylamine (DIPEA)	84.19145	6.395602
glycine	0.003459	-8.1756
N8-Acetylspermidine	18.72085	4.226574
n-Hexanamide	0.470374	-1.08812
N-Methylhexanamide	0.463854	-1.10826
Oleamide	7.660355	2.937411
Palmitoylcarnitine	0.013476	-6.21351
P-DMEA	0.017528	-5.83421
Phosphoric acid	2.460913	1.299194
Platelet-activating factor	0.040504	-4.6258
Propionylcarnitine	0.028996	-5.10802
PROPOFOL GLUCURONIDE	0.00819	-6.93194
stearoylcarnitine	0.009967	-6.6486
Taurine	0.08628	-3.53484
Tetramethylpyrazine	0.270892	-1.88421
THTC	0.216245	-2.20926
Timonacic	0.098814	-3.33914
trans-3-Indoleacrylic acid	0.334997	-1.57778
Trifluoroacetic acid	0.298004	-1.7466

Uridine 5-diphosphogalactose	0.483198	-1.04931
ZV4	0.346605	-1.52864

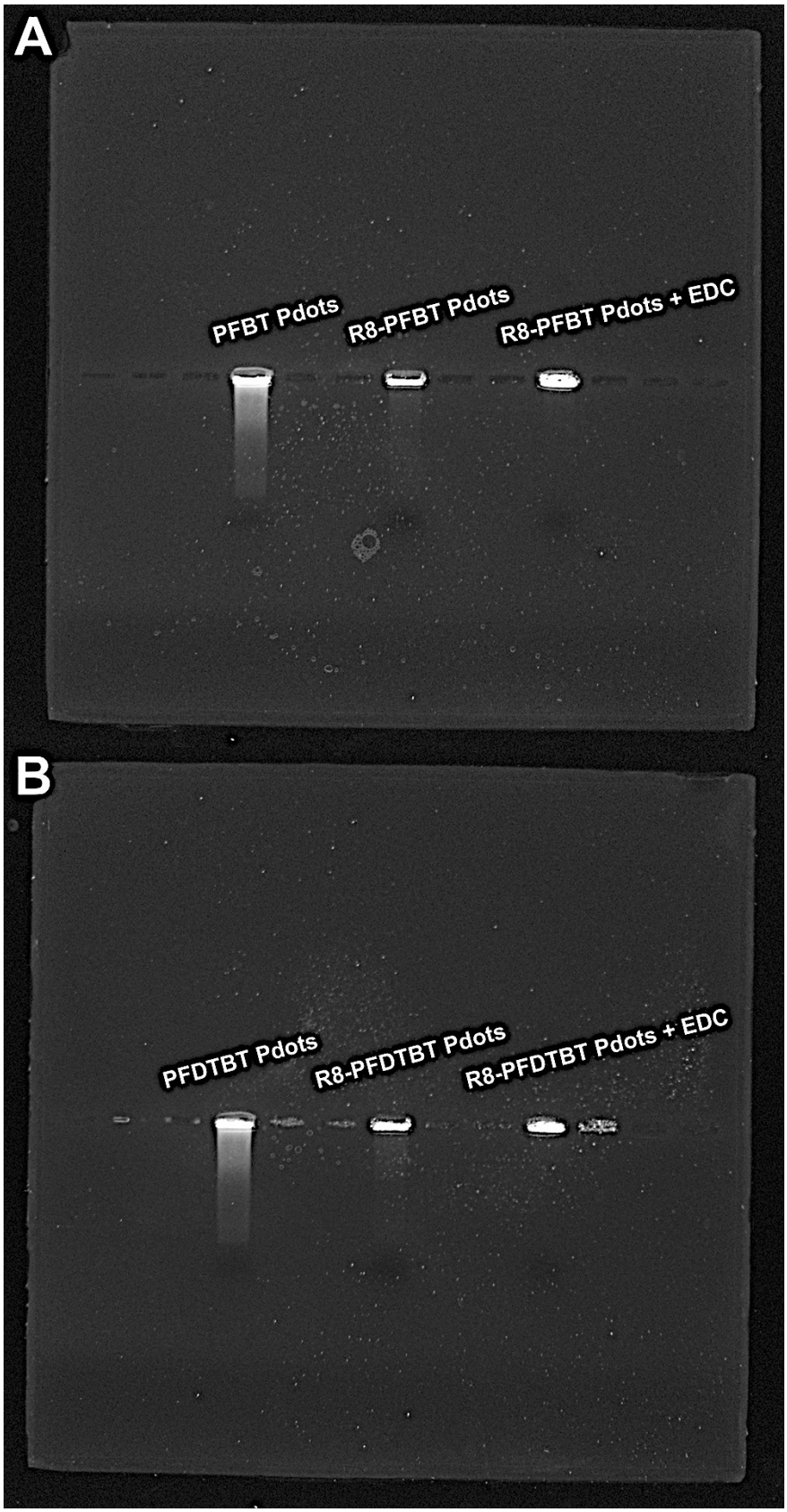

Supporting Figures

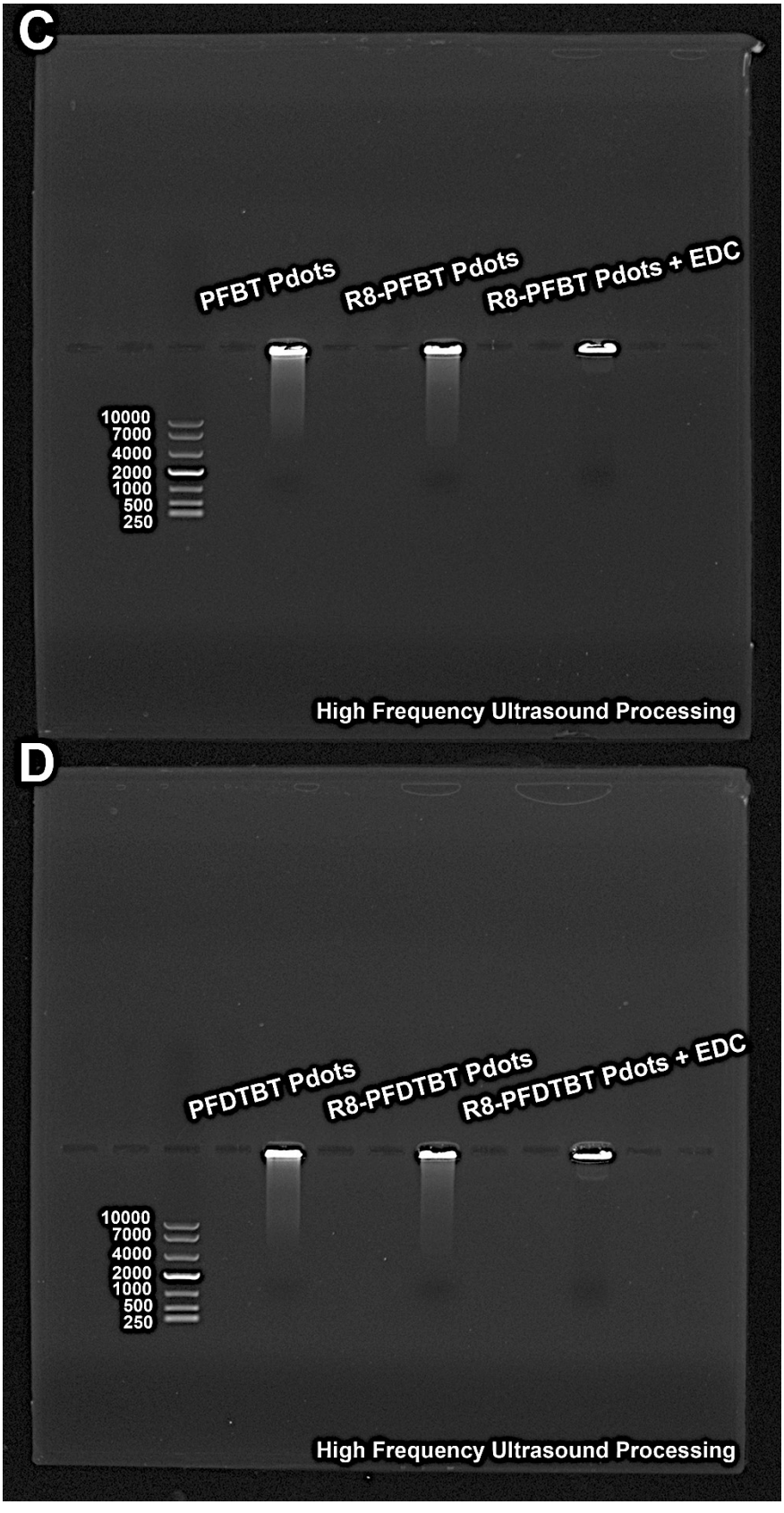
C
PFBT Pdots
R8-PFBT Pdots
R8-PFBT Pdots + EDC
10000
7000
4000
2000
1000
500
250
High Frequency Ultrasound Processing
D
PFDTBT Pdots
R8-PFDTBT Pdots
R8-PFDTBT Pdots + EDC
10000
7000
4000
2000
1000
500
250
High Frequency Ultrasound Processing

Figure S1. Original Electrophoretic Pictures of Pdots and R8-Pdots.

A. PFBT Pdots/ R8-PFBT Pdots/ R8-PFBT Pdots+EDC without high-frequency ultrasound processing after electrostatic adsorption. B. PFDTBT Pdots/ R8-PFDTBT Pdots/ R8-PFDTBT Pdots+EDC without high-frequency ultrasound processing after electrostatic adsorption. C. PFBT Pdots/ R8-PFBT Pdots/ R8-PFBT Pdots+EDC processed with high-frequency ultrasound. D. PFDTBT Pdots/ R8-PFDTBT Pdots/ R8-PFDTBT Pdots+EDC processed with high-frequency ultrasound.

The electrophoresis results show that the band of R8-Pdots after the high-frequency ultrasound is spread longer and mainly concentrated in the small molecule region. On the other hand, R8-Pdots+EDC, chemically bonded together in the presence of EDC, do not show a similar pattern.

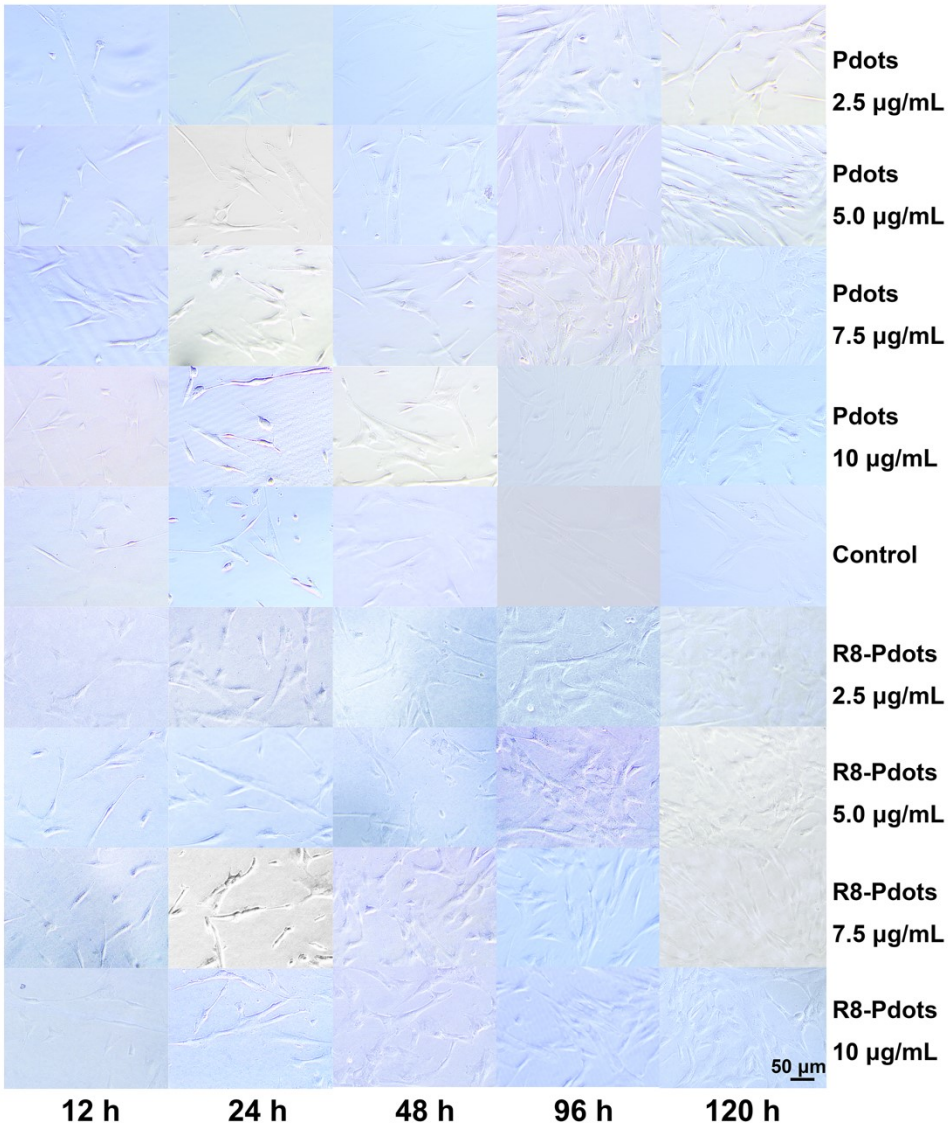

Figure S2. The appearance of MSCs after co-culture with PFBT Pdots & R8-PFBT Pdots.

MSCs morphology under the light microscope. When the concentration of R8-Pdots was lower than 10 μg/mL, the appearance of the cells was not affected, and the MSCs still showed the cellular morphology of a long spindle. The scale bar is 50 μm.

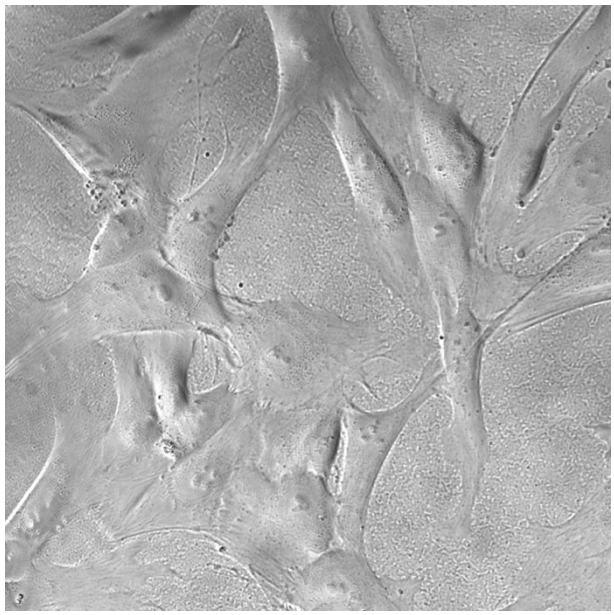

Figure S3. Non-specific dissection of MSCs co-cultured with R8-PFBT Pdots.

Notably, when the concentration of R8-PFBT Pdots was more than 10 μg/ml, after a certain period of co-culture (the starting time node was calculated from the end of incubation), the coculture time > 4 h, R8-PFBT Pdots would peel MSCs cells away from the surface of the dish but did not kill primary MSCs cells. For example, the MSCs remain viable when the suspended cell mass stripped, as described above, is collected, and transferred to a new culture flask without the R8-PFBT Pdots medium. The phenomenon would gradually become evident with the increasing concentration of the initial incubation solution.

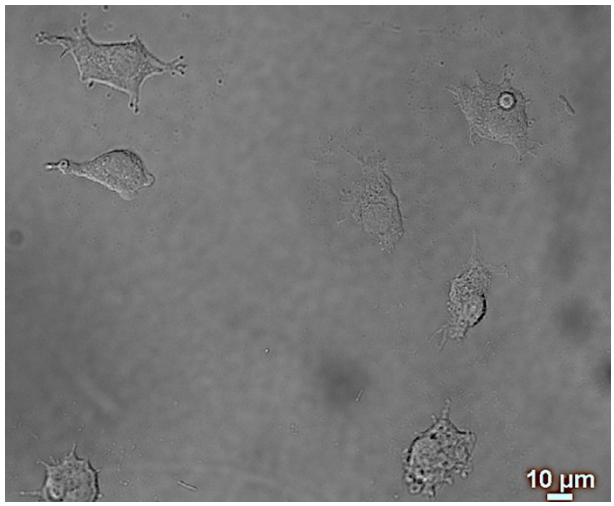

Figure S4. Vacuolar-like degeneration of HUVECs.

When the concentration of R8-PFDTBT Pdots was higher than 7.5 μg/ml, there was vacuolar-like degeneration of labelled target cells after prolonged culture. Note: scale bar: 10 μm.

To address the above two issues (Fig. S3 & S4), we used Wharton's Jelly at a concentration of 1 mg/ml to coat the surface of the culture dish. In addition, since R8 is conjugated with Pdots through

electrostatic forces and the large number of "cations " contained within Wharton's Jelly coated between the medium and the culture dish, these cations would competitively bind with R8 to the dye-incorporated PSMA inside, resulting in the poor colloidal stability of R8-Pdots, so that free Pdots or R8-Pdots produce aggregation, attachment on the surface of the culture dish or non-specific adsorption to the cell membrane, Produce a background interfering signal upon imaging or detection. At the same time, for any exogenous fluorescent probe, the labelled probe will enter into the mitotically formed progeny cells with the continued proliferation of the target cells, thus decreasing the number of labelled probes and the reduction of fluorescence intensity in the progeny cells. In addition, they showed vacuole-like degeneration under a light microscope (Fig. S4), and microscopically observable vacuole-like deterioration also became more significant with the increase of initial concentration of R8-Pdots label solution and reproductive passage (P). Therefore, to balance the above factors, we finally chose 5 μg / ml of R8-Pdots (R8-PFBT Pdots & R8-PFDTBT Pdots) as the initial incubation concentration for subsequent experiments, at which non-specific stripping of MSCs and vacuole like deformation of HUVECs could be avoided.

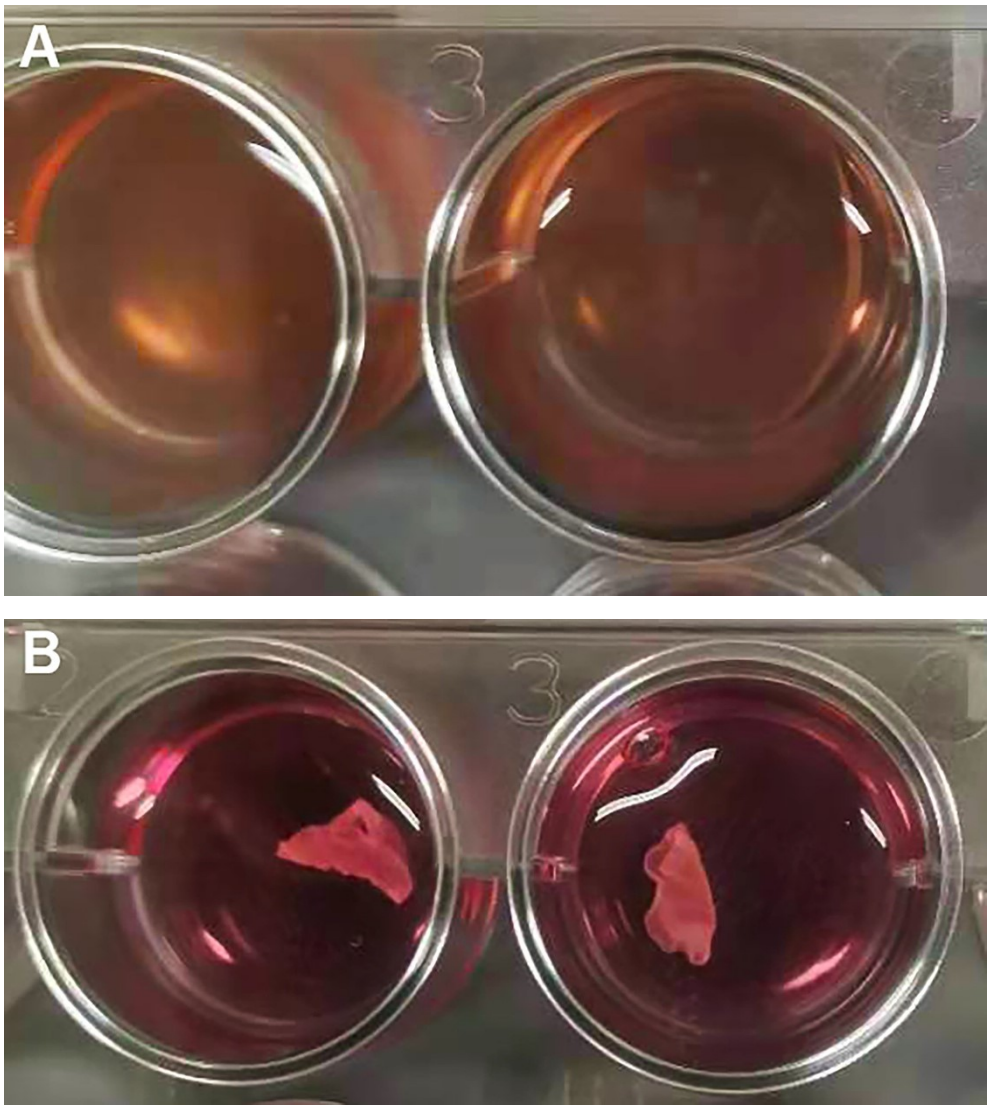

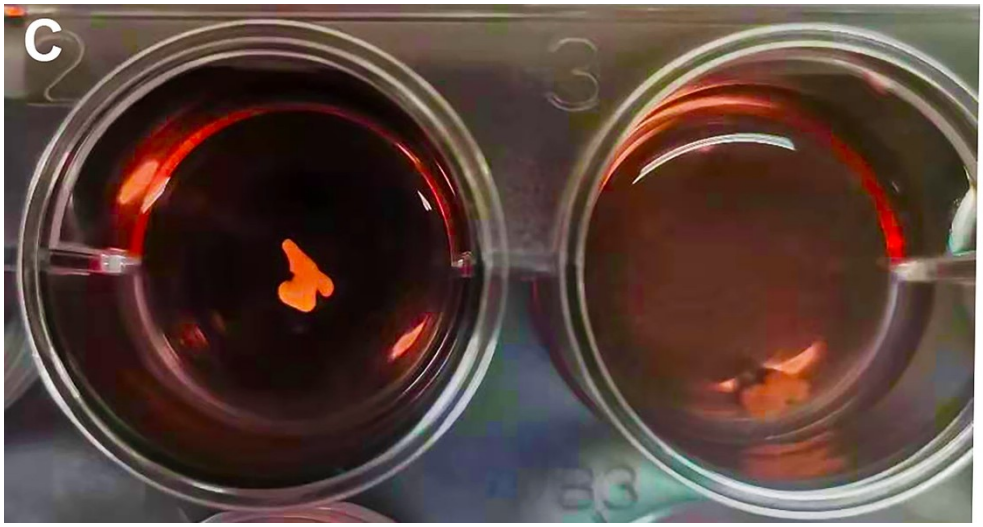

Figure S5. Reproducibility test of Liver Organoid Cultures.

A. After 24 h of co-cultured.

B. After 48 h of co-cultured.

C. After 72 h of co-cultured.

The whole process of organoid self-assembly. With the improved culture protocol, the success rate of liver organoid culture can be as high as 97 %.

Figure S6. Validate the "skeleton" function of HUVECs.

We replaced the extracted primary venous endothelial cells with bioengineered immortal endothelial cells, which have poor adhesion and lack part of the molecular phenotype of the primary cells, to verify the finding in the biological skeleton function of HUVECs further. The results suggest that the liver organoid structure with spatial structure could not be formed in vitro, and the general shape only stayed in the starting state of the self-assembly process of 24 h ~ 48 h.

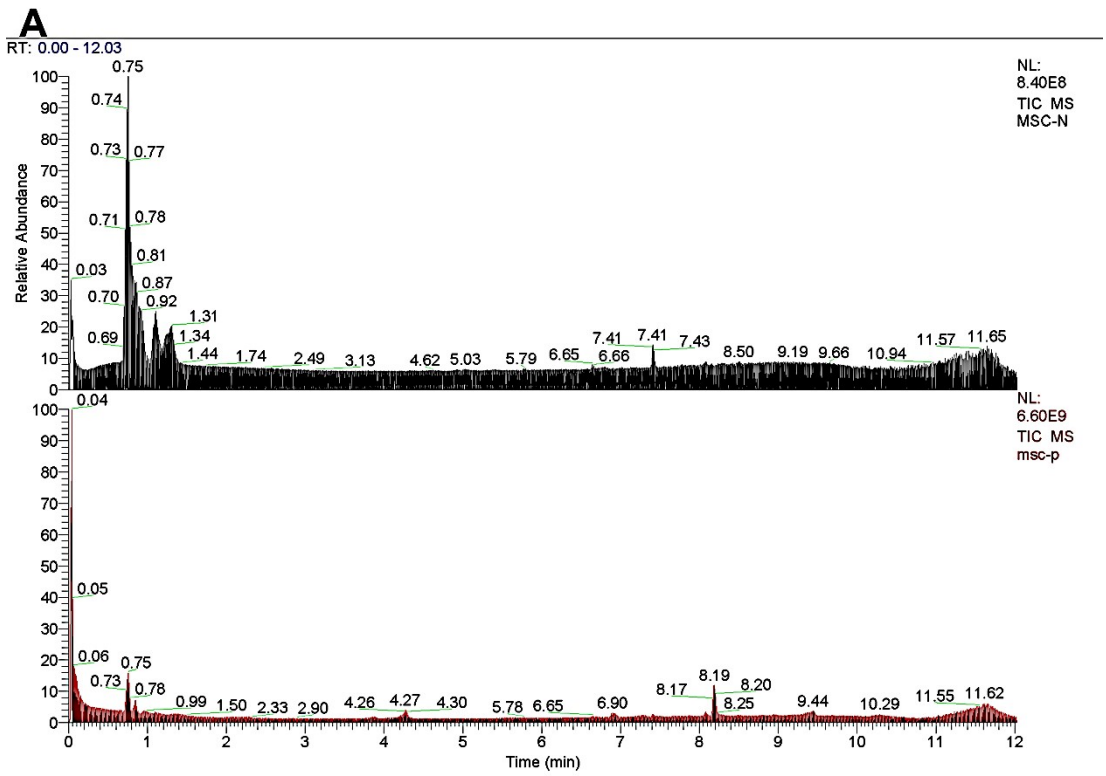
A
RT: 0.00 - 12.03
NL:
8.40E8
TIC MS
MSC-N
NL:
6.60E9
TIC MS
msc-p
Relative Abundance
Time (min)

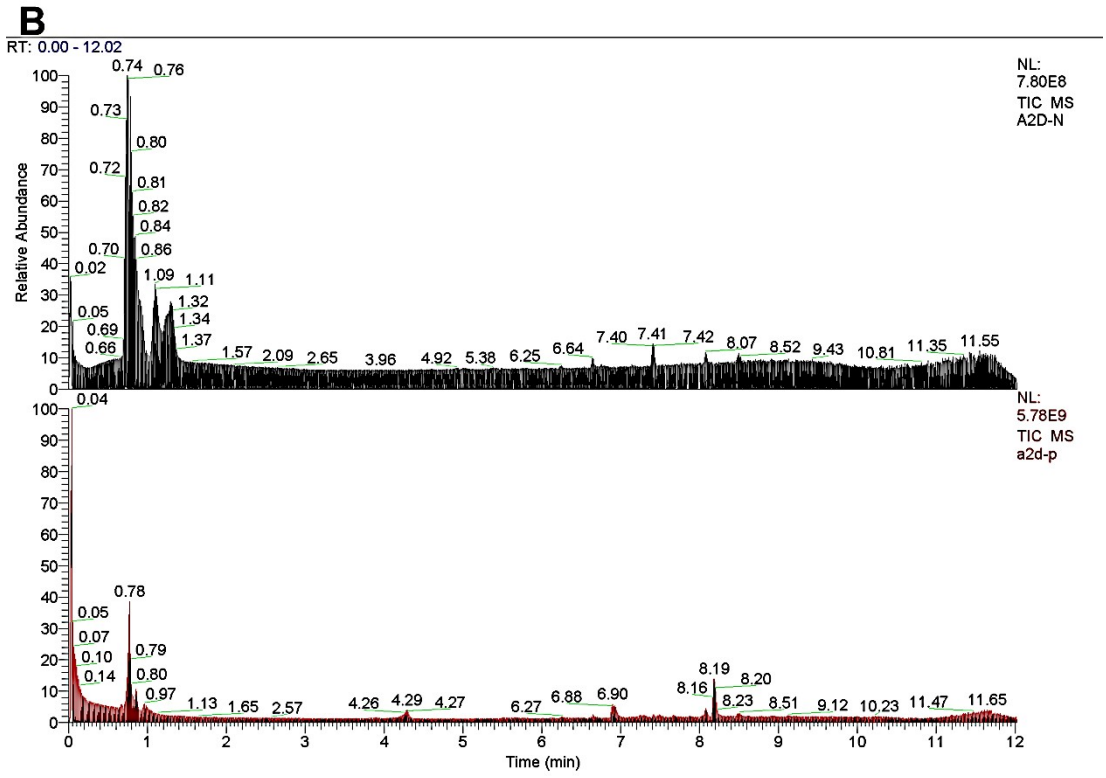
B
RT: 0.00 - 12.02
NL:
7.80E8
TIC MS
A2D-N
NL:
5.78E9
TIC MS
a2d-p
Relative Abundance
Time (min)

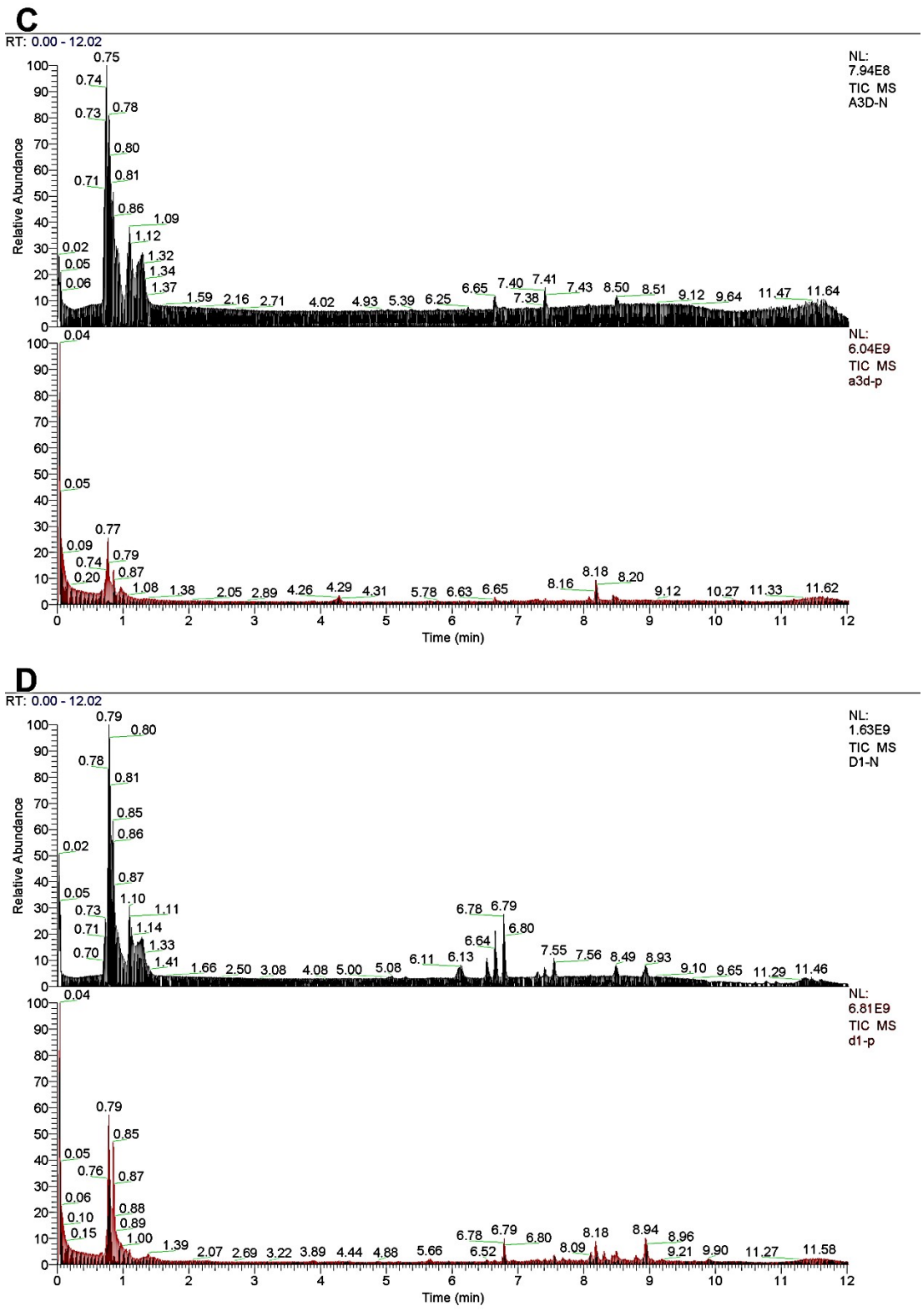

Figure S7. Ion chromatogram of the test sample.

A. MSCs.

B. 2D-culture induced differentiation of hepatocyte-like cells.

C. 3D-liver organoid cultivation.

D. The normal liver tissue cells.

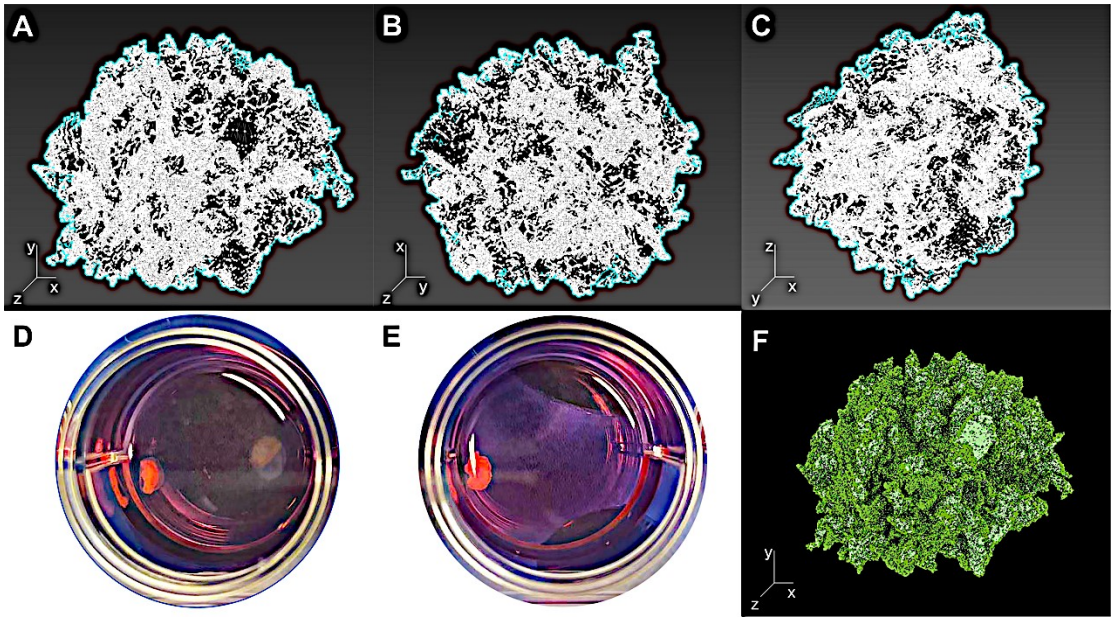

Figure S8. Point cloud reconstruction of liver organoid cell clusters at 96 h.

A. Orthopantomogram.

B. Lateral view.

C. Top view.

D. Liver organoids cocultured after 72 h in vitro.

E. Liver organoids cocultured after 96 h in vitro. Compared with Fig. S8D, the macromorphology of organoids hardly changed after 72 hours of co-culture.

F. Reconstructed image from orthopantomogram. Reconstructed image of liver organoid cell clusters in Fig. S8E.

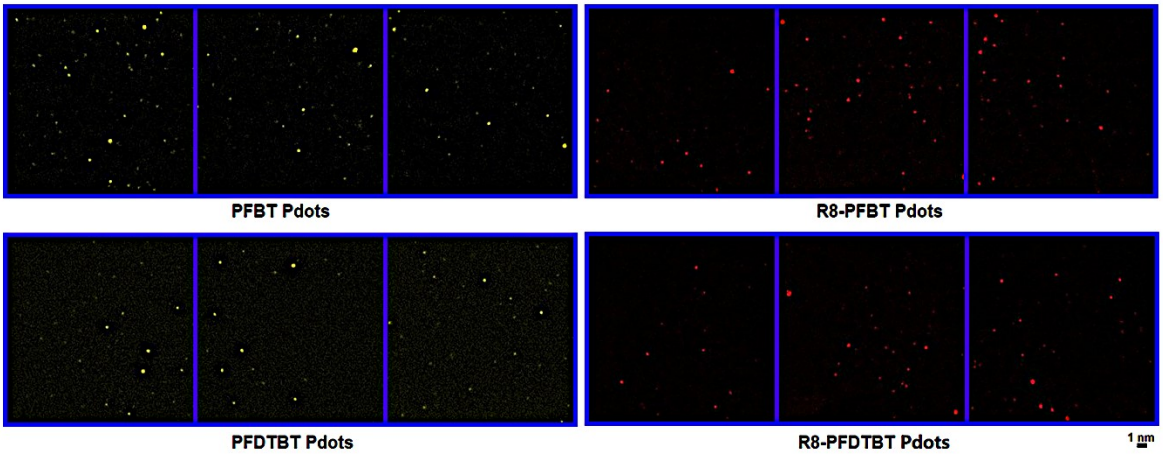

Figure S9. Single particle fluorescence images of Pdots & R8-Pdots.

Upper. PFBT Pdots & R8- PFBT Pdots.

Lower. PFDTBT Pdots & R8- PFDTBT Pdots.

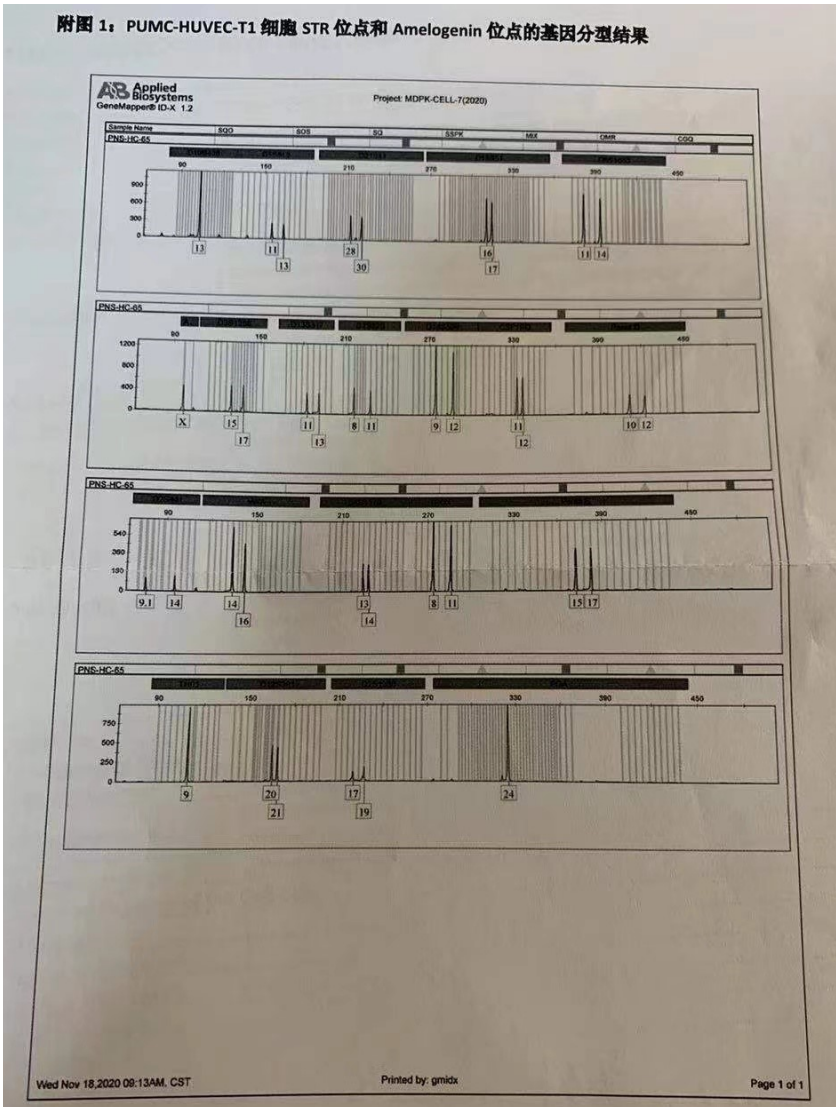

Figure S10. The bioengineered immortal endothelial cells.

STR locus and Amelogenin locus identification diagram of this type of cells provided by the technical department of ProCell®.

References

1. Z. Zhang, Y. Wu, N. Lin, S. Yin and Z. Meng, *ACS Appl Mater Interfaces*, 2022, **14**, 7717-7730.
2. K. Sun, Y. Tang, Q. Li, S. Yin, W. Qin, J. Yu, D. T. Chiu, Y. Liu, Z. Yuan, X. Zhang and C. Wu, *ACS Nano*, 2016, **10**, 6769-6781.
3. D. Balboa, T. Barsby, V. Lithovius, J. Saarimaki-Vire, M. Omar-Hmeadi, O. Dyachok, H. Montaser, P. E. Lund, M. Yang, H. Ibrahim, A. Naatanen, V. Chandra, H. Vihinen, E. Jokitalo, J. Kvist, J. Ustinov, A. I. Nieminen, E. Kuuluvainen, V. Hietakangas, P. Katajisto, J. Lau, P. O. Carlsson, S. Barg, A. Tengholm and T. Otonkoski, *Nat Biotechnol*, 2022, **40**, 1042-1055.
4. K. Takeishi, A. Collin de l'Hortet, Y. Wang, K. Handa, J. Guzman-Lepe, K. Matsubara, K. Morita, S. Jang, N. Haep, R. M. Florentino, F. Yuan, K. Fukumitsu, K. Tobita, W. Sun, J. Franks, E. R. Delgado, E. M. Shapiro, N. A. Fraunhoffer, A. W. Duncan, H. Yagi, T. Mashimo, I. J. Fox and A. Soto-Gutierrez, *Cell Rep*, 2020, **31**, 107711.
5. T. Takebe, K. Sekine, M. Enomura, H. Koike, M. Kimura, T. Ogaeri, R. R. Zhang, Y. Ueno, Y. W. Zheng, N. Koike, S. Aoyama, Y. Adachi and H. Taniguchi, *Nature*, 2013, **499**, 481-484.
6. T. Takebe, R. R. Zhang, H. Koike, M. Kimura, E. Yoshizawa, M. Enomura, N. Koike, K. Sekine and H. Taniguchi, *Nat Protoc*, 2014, **9**, 396-409.
7. O. Pande, H. Makaram and R. Swaminathan, *Annu Int Conf IEEE Eng Med Biol Soc*, 2022, **2022**, 3959-3962.
8. D. S. Umbaugh, R. P. Soder, N. T. Nguyen, O. Adelusi, D. R. Robarts, B. Woolbright, L. Duan, S. Abhyankar, B. Dawn, U. Apte, H. Jaeschke and A. Ramachandran, *Arch Toxicol*, 2022, DOI: 10.1007/s00204-022-03372-5.
9. M. Z. C. Hatit, M. P. Lokugamage, C. N. Dobrowolski, K. Paunovska, H. Ni, K. Zhao, D. Vanover, J. Beyersdorf, H. E. Peck, D. Loughrey, M. Sato, A. Cristian, P. J. Santangelo and J. E. Dahlman, *Nat Nanotechnol*, 2022, **17**, 310-318.
10. H. Koike, K. Iwasawa, R. Ouchi, M. Maezawa, K. Giesbrecht, N. Saiki, A. Ferguson, M. Kimura, W. L. Thompson, J. M. Wells, A. M. Zorn and T. Takebe, *Nature*, 2019, **574**, 112-116.
11. K. Lewis, M. Yoshimoto and T. Takebe, *Stem Cell Res Ther*, 2021, **12**, 139.
12. W. L. Thompson and T. Takebe, *Dev Growth Differ*, 2021, **63**, 47-58.
13. T. Wang, L. Zhang, W. Liang, S. Liu, W. Deng, Y. Liu, Y. Liu, M. Song, K. Guo and Y. Zhang, *Autophagy*, 2022, **18**, 1433-1449.
14. V. Francia, K. Yang, S. Deville, C. Reker-Smit, I. Nelissen and A. Salvati, *ACS Nano*, 2019, **13**, 11107-11121.
15. Z. Leon, J. C. Garcia-Canaveras, M. T. Donato and A. Lahoz, *Electrophoresis*, 2013, **34**, 2762-2775.
16. H. P. Benton, J. Ivanisevic, N. G. Mahieu, M. E. Kurczy, C. H. Johnson, L. Franco, D. Rinehart, E. Valentine, H. Gowda, B. K. Ubhi, R. Tautenhahn, A. Gieschen, M. W. Fields, G. J. Patti and G. Siuzdak, *Anal Chem*, 2015, **87**, 884-891.
17. J. Ivanisevic, Z. J. Zhu, L. Plate, R. Tautenhahn, S. Chen, P. J. O'Brien, C. H. Johnson, M. A. Marletta, G. J. Patti and G. Siuzdak, *Anal Chem*, 2013, **85**, 6876-6884.
18. R. J. DeBerardinis and K. R. Keshari, *Cell*, 2022, **185**, 2678-2689.

19. N. Ma, S. Li, C. Lin, X. Cheng and Z. Meng, *Bioengineered*, 2021, **12**, 6434-6447.
20. V. Bagalkot, L. Zhang, E. Levy-Nissenbaum, S. Jon, P. W. Kantoff, R. Langer and O. C. Farokhzad, *Nano Lett*, 2007, **7**, 3065-3070.
21. J. Zhang, L. Hou, Z. Zuo, P. Ji, X. Zhang, Y. Xue and F. Zhao, *Nat Biotechnol*, 2021, **39**, 836-845.